

## Hands on LUCIFER: from assembly, operation and characterization of bolometric detectors, to calibration and definition of the power discrimination

---

### M. Nebot-Guinot<sup>\*†</sup>

*Instituto de Física Corpuscular (IFIC), CSIC & Universitat de València  
Calle Catedrático José Beltrán, 2, 46980 Paterna, Valencia, Spain  
E-mail: [miquel.nebot@ific.uv.es](mailto:miquel.nebot@ific.uv.es)*

### Mateusz Kaczmarski<sup>‡</sup>

*Institute of Physics, University of Szczecin, ul. Wielkopolska 15, 70-451 Szczecin, Poland  
E-mail: [mkaczmarskil@gmail.com](mailto:mkaczmarskil@gmail.com)*

### L. Pattavina<sup>§</sup>

*INFN - Laboratori Nazionali del Gran Sasso, Assergi (L'Aquila) I-67010 - Italy  
E-mail: [luca.pattavina@lngs.infn.it](mailto:luca.pattavina@lngs.infn.it)*

The students will carry out the experimental activity in the frame of the LUCIFER project. The activity foresees the assembly and operation of bolometric detectors. In the specific, the students will directly put hands on the detector, designing and constructing a scintillating bolometer. The detector will be installed in a dilution refrigerator and operated at 10 mK. Finally, the students will analyze some preliminary data from the running setup.

*Gran Sasso Summer Institute 2014 Hands-On Experimental Underground Physics at LNGS - GSSI14,  
22 September - 03 October 2014  
INFN - Laboratori Nazionali del Gran Sasso, Assergi, Italy*

---

\*Speaker.

†GSSI Student.

‡GSSI Student.

§Advisor.

## 1. Introduction

Neutrinoless double beta decay (0νDBD) is one of the most important nuclear processes investigated in the recent years. Great effort was undertaken by the Particle Physics community to research for the best technology for investigating such rare decay. 0νDBD is forbidden by Standard Model (SM), because of the lepton number violation, and the observation of this decay would imply the Majorana nature of neutrinos [4]. Furthermore the experimental observation of this rare process, and the measurement of its half-life would also give information on the neutrino mass scale. There are various existing and upcoming experimental techniques devoted to the 0νDBD detection. Among the most promising there is one based on bolometers adopted by experiments such as CUORE0 [3] and LUCIFER [4].

In this work we report on an R&D activity carried out in the frame of the LUCIFER project. LUCIFER aims at deploying the first array of enriched scintillating bolometers for the investigation of DBD in  $Zn^{82}Se$  ( $Zn^{100}MoO_4$ ) crystals. Scintillating bolometers combine: an excellent energy resolution [8], high detection efficiency [9], particle discrimination [7], and a wide choice of absorber materials [2]. In this bolometric approach the crystal acts as the source and the detector at the same time. The experimental set-up consists of a main absorber, the scintillating crystal (heat channel) and of a light detector, namely a Germanium wafer (light channel). The simultaneous read-out of the two channels allows the identification of the nature of the interacting particle, leading to an abrupt background suppression in the region of interest.

Such detectors can meet the requirements for zero-background investigations, thus can provide a high experimental sensitivity [2] and provide the possibility of investigating the inverted hierarchy region of neutrino mass.

## 2. Assembly

In order to be able to detect such rare process it is mandatory to reduce any background that can mask the investigated signal. For this reason the detectors have to be built in clean environment using extremely pure components, with extra care for transport and assembly. To maintain the radiopurity, high quality copper elements were used as mounting structure for ZnSe and ZnMoO<sub>4</sub> crystals using Teflon as detector holders.

The first step of the bolometer assembly was coupling Neutron Transmutation Doped (NTD) thermistors to the surface of the crystal and of the Germanium slab with very thin epoxy glue layer, using special dosing system developed by LUCIFER. In Fig. 1 is clearly visible the various NTDs (different types) for each sensor coupled to the surface. This gluing procedure is made under the microscope for  $\mu m$  precision in the NTD-crystal coupling for the optimal phonon transmission without dissipation. Next step was mounting the crystals on a copper frame with Teflon thermal insulators and connecting 25  $\mu m$  thick gold wires for the channel read-out. The wiring was also made under the microscope due to its thickness and fragility, then crimped to ensure the electrical connectivity. In Fig. 1 the gold wires are visible going from the NTDs to the copper pins in each side. The last part consisted in mounting the scintillating crystal and the Ge slab, facing each other

and adding a reflecting foil around detector in order to increase the light collection efficiency. The module (scintillating crystal + light detector) was housed in a dilution refrigerator and operated at a cryogenic temperature of  $\sim 10mK$ .

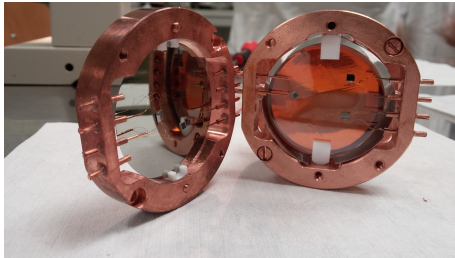


Figure 1: ZnSe bolometer assembled. On the left is the Ge light detector (mirror appearance) and on the right the ZnSe crystal (translucent orange).

### 3. Characterization

In the following we report on the characterization of a  $ZnMoO_4$  crystal operated as scintillating bolometer inside the  $^3He/^4He$  dilution refrigerator in the Hall C of the Gran Sasso Underground Laboratory.

In order to ensure the best performance and operation of the detectors, a characterization of its optimum working point is needed. This is done changing the bias voltage of the thermistor of the heat detector ( $ZnMoO_4$ ) and the light detector (Ge), and looking into the response at each operational voltage. This is accomplished by means of a fixed resistance (heater), directly coupled to the absorber through which it is possible to dissipate a known joule power into the crystal in a manner perfectly similar to a particle energy deposit.

Once the responses of the detector are collected for the different applied voltage, it is possible to produce the *Load Curve*. This describes the detector response to a given signal amplitude as function of the operational voltage ( Fig. 2 ). Ideally we would like to have the largest response, that means the highest pulse voltage drop. The actual *optimum working point* is chosen by investigating the signal-to-noise ratio. Since the electronic sources of noise decrease with the resistance of the bolometer (Johnson noise), the best working point corresponds to a bias voltage slightly higher than the one corresponding to the optimum point.

### 4. Data taking

After determining the parameters for the best working point, we set those conditions to the detector and took some data (R1) with a calibration source (Thorium) to see the detector performance. Furthermore we took various runs of data according different operating conditions of the detectors (Table 1). In those runs we have changed the condition of the environment, basically warming up the cryostat and changing the bias voltage on the thermistor to set a worse working

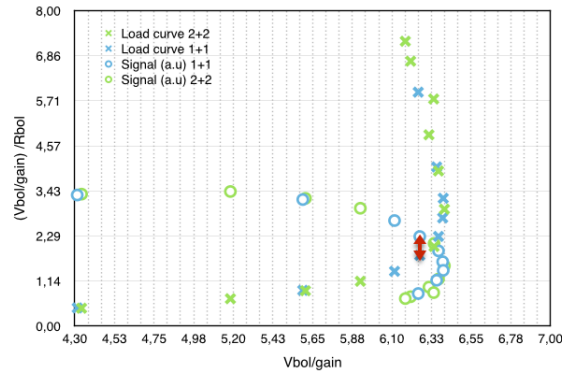


Figure 2:  $ZnMoO_4$  bolometer characterization. It is shown the behavior and response of the heat detector. It is also marked with an arrow the best working point according to the criteria explained above.

Parameter	R1	R2	R3
Temperature	$\sim 11mK$	$\sim 11mK$	$\sim 11.5mK$
Heat detector			
Load configuration	RL 1+1	RL 1+1	RL 2+2
Bias Voltage(mV)	3597	14819	9014
Bolometer Resistance (MOhm)	3.4	1.0	2.6
Bolometer Current (nA)	3.58	14.8	4.5
Calibration source	$^{228}Th$	$^{228}Th$	$^{228}Th$

Table 1: Detector performance for each data set.

point of the bolometer. This allows us to compare the behavior of the detector with the best conditions achievable and how this affects the energy resolution and the capability to distinguish the nature of the interacting particle (Discrimination Power).

## 5. Analysis

Data processing, from raw data to the final energy spectra, is carried out following the procedures described in details in [1]. The amplitude of the acquired pulses is estimated by means of the Optimum Filter technique [6], that maximizes the signal to noise ratio. Changes in the stability of the detectors are corrected using the reference signals generated by the heater. Pulse shape cuts are applied to suppress pile-up or noisy or spurious events that can produce a broadening or a deformation of the energy resolution. Those cuts are based on the shape parameter comparison, that means the difference between every single pulse and an average reference one. Selecting the event which deposited energy in the main absorber ( $ZnMoO_4$ ) and the events produced in the Light Detector, which are synchronized, it is possible to produce scatter plots like the one shown in Fig. 3. Where the different behavior depending on the nature of the energy deposit is clearly visible. The light yield, as well as the different time development of pulses produced by  $\alpha$  and  $\beta/\gamma$  particles, constitute two semi-independent discrimination tools that can provide an almost complete rejection of the  $\alpha$  background [5]. Finally, the energy calibration is performed by means of known gamma lines produced by a  $^{228}Th$  source.

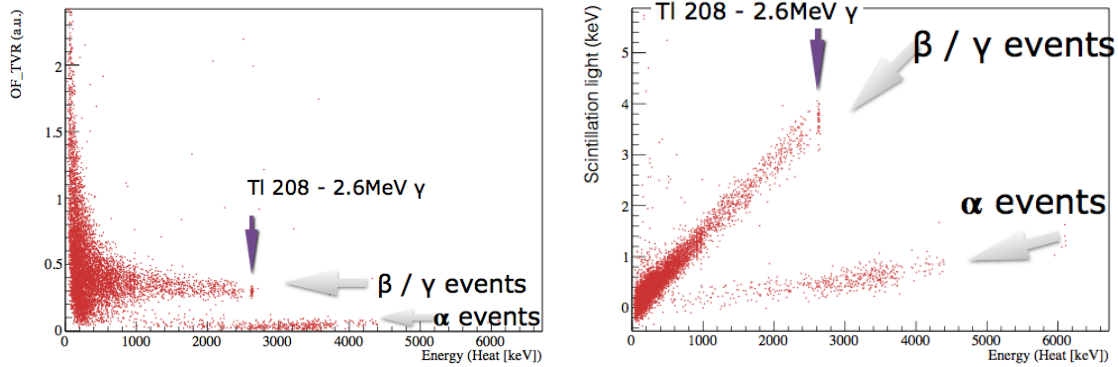


Figure 3: Shape parameter versus energy deposited (left) and scintillation light detected versus energy deposited (right) from the first data set conditions (R1).

### 5.1 Energy resolution

Using the data preprocessed it is possible to plot the energy spectrum of  $\beta/\gamma$  events and see the various peaks produced by the gamma calibration source. The most intense line next to the region of interest for DBD experiments using Molybdenum is the 2.6 MeV emission of  $^{208}\text{Tl}$ , produced by the decay chain of  $^{228}\text{Th}$ , see Fig. 4. Fitting a Gaussian to this peak, the energy resolution of the detector can be estimated. As we took data in different configurations we could see how the FWHM energy resolution varies with the performance of the detector from 8 keV up to 25 keV.

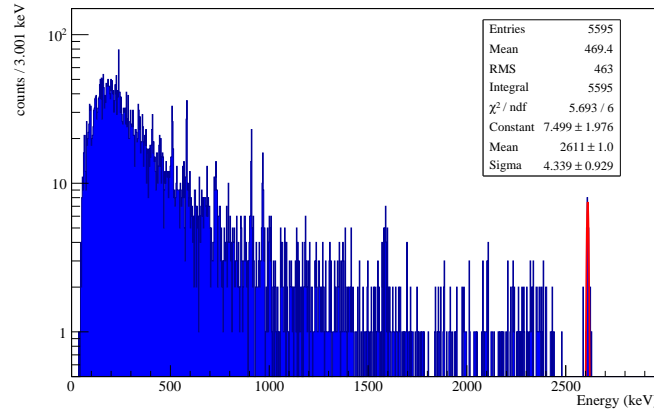


Figure 4:  $\beta/\gamma$  Energy spectrum from the first data set conditions (R1). In the inset are shown the fitting parameters for the gamma line at 2.6 MeV

### 5.2 Power discrimination

To evaluate the discrimination capability, we performed a Gaussian fit of the two distributions ( $\beta/\gamma$  and  $\alpha$ ) using two different variables: the light detected in the light channel and a pulse shape parameter of the event detected by the heat channel. From the fits we derived the mean value ( $\mu$ ) and the standard deviation ( $\sigma$ ) of the  $\alpha$  and  $\beta/\gamma$  distributions.

$$DP = \frac{\mu_{\beta/\gamma} - \mu_{\alpha}}{\sqrt{\sigma_{\beta/\gamma}^2 - \sigma_{\alpha}^2}} \quad (5.1)$$

In Fig.5 are shown two scatter plots for two different working temperatures of the bolometer. It is remarkably visible how the discrimination power is dependent on the temperature of the bolometer. For large operating currents of the thermal sensor, thus higher temperature, there is a faster pulse development (shorter rise time) that fades away any difference between alpha particles and beta/gamma see Fig. 5a. While for smaller current, thus colder temperature, there is an enhancement of the difference between the thermal pulses of alpha and beta/gamma particles, see Fig. 5b. This behaviour is in full agreement with [10], where the mechanism for the different pulse shape for different interacting particles is described.

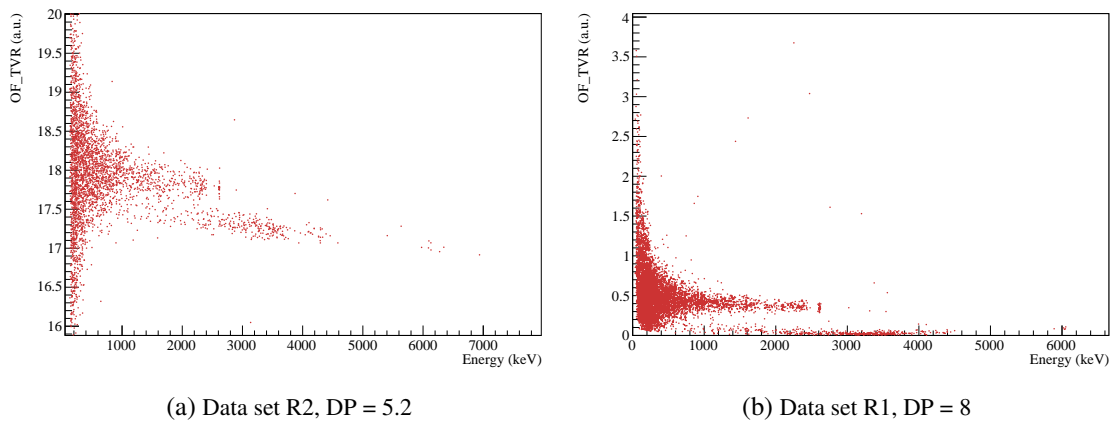


Figure 5: Discrimination Power variation with running conditions.

## 6. Conclusions

During this experience we have build a scintillation bolometer using the technique developed by the LUCIFER collaboration. We have characterized those detectors and operate them. After all we have been able to analyze data taken with a prototype detector and show how powerful is this detector for rejecting backgrounds, using both the light channel but also the heat one.

## References

- [1] E. Andreotti, C. Arnaboldi, F.T. Avignone, M. Balata, I. Bandac, et al.  $^{130}\text{Te}$  Neutrinoless Double-Beta Decay with CUORICINO. *Astropart.Phys.*, 34:822–831, 2011.
- [2] D.R. Artusa et al. Exploring the Neutrinoless Double Beta Decay in the Inverted Neutrino Hierarchy with Bolometric Detectors. *Eur.Phys.J.*, C74(10):3096, 2014.
- [3] D.R. Artusa et al. Initial performance of the CUORE-0 experiment. *Eur.Phys.J.*, C74(8):2956, 2014.
- [4] J.W. Beeman, F. Bellini, P. Benetti, L. Cardani, N. Casali, et al. Current Status and Future Perspectives of the LUCIFER Experiment. *Adv.High Energy Phys.*, 2013:237973, 2013.

- [5] J.W. Beeman, F. Bellini, C. Brofferio, L. Cardani, N. Casali, et al. Performances of a large mass ZnMoO<sub>4</sub> scintillating bolometer for a next generation 0νDBD experiment. *Eur.Phys.J.*, C72:2142, 2012.
- [6] J.W. Beeman, F. Bellini, L. Cardani, N. Casali, I. Dafinei, et al. Performances of a large mass ZnSe bolometer to search for rare events. *JINST*, 8:P05021, 2013.
- [7] J.W. Beeman, F. Bellini, L. Cardani, N. Casali, S. Di Domizio, et al. New experimental limits on the alpha decays of lead isotopes. *Eur.Phys.J.*, A49:50, 2013.
- [8] J.W. Beeman, M. Biassoni, C. Brofferio, C. Bucci, S. Capelli, et al. First measurement of the partial widths of <sup>209</sup>Bi decay to the ground and to the first excited states. *Phys.Rev.Lett.*, 108:062501, 2012.
- [9] C. Bucci, S. Capelli, M. Carrettoni, M. Clemenza, O. Cremonesi, et al. Background study and Monte Carlo simulations for large-mass bolometers. *Eur.Phys.J.*, A41(2):155–168, 2009.
- [10] L. Gironi. Pulse Shape Analysis with scintillating bolometers. *Nucl.Instrum.Meth.*, A718:546–549, 2013.